Coastal Engineering 57 (2010) 539–552

Contents lists available at ScienceDirect

Coastal Engineering

journal homepage: www.elsevier.com/locate/coastaleng

Increasing wave heights and extreme value projections: The wave climate of the U.S. Pacific Northwest

Peter Ruggiero [a,*], Paul D. Komar [b], Jonathan C. Allan [c]

[a] Department of Geosciences, Oregon State University, Corvallis, OR 97331, USA
[b] College of Oceanic & Atmospheric Sciences, Oregon State University, Corvallis, OR 97331, USA
[c] Coastal Field Office, Oregon Dept. of Geology and Mineral Industries, 313 SW 2nd, Newport, OR 97365, USA

ARTICLE INFO

Article history:
Received 2 February 2009
Received in revised form 5 December 2009
Accepted 18 December 2009
Available online 18 January 2010

Keywords:
Coastal hazards
Coastal engineering design
Extreme values
Increasing storminess
Lognormal distribution
Oregon
Significant wave height
Washington

ABSTRACT

Deep-water wave buoy data offshore from the U.S. Pacific Northwest (Oregon and Washington) document that the annual averages of deep-water significant wave heights (SWHs) have increased at a rate of approximately 0.015 m/yr since the mid-1970s, while averages of the five highest SWHs per year have increased at the appreciably greater rate of 0.071 m/yr. Histograms of the hourly-measured SWHs more fully document this shift toward higher values over the decades, demonstrating that both the relatively low waves of the summer and the highest SWHs generated by winter storms have increased. Wave heights associated with higher percentiles in the SWH cumulative distribution function are shown to be increasing at progressively faster rates than those associated with lower percentiles. This property is demonstrated to be a direct result of the probability distributions for annual wave climates having lognormal- or Weibull-like forms in that a moderate increase in the mean SWH produces significantly greater increases in the tail of the distribution. Both the linear regressions of increasing annual averages and the evolving probability distribution of the SWH climate, demonstrating the non-stationarity of the Pacific Northwest wave climate, translate into substantial increases in extreme value projections, important in coastal engineering design and in quantifying coastal hazards. Buoy data have been analyzed to assess this response in the wave climate by employing various time-dependent extreme value models that directly compute the progressive increases in the 25- to 100-year projections. The results depend somewhat on the assumptions made in the statistical procedures, on the numbers of storm-generated SWHs included, and on the threshold value for inclusion in the analyses, but the results are consistent with the linear regressions of annual averages and the observed shifts in the histograms.

1. Introduction

In recent decades increases in wave heights generated by the most intense storms have occurred in both the North Atlantic and the Northeast Pacific. In the Atlantic this increase has been documented by the Seven Stones light vessel offshore from the southwest coast of England (Carter and Draper, 1988; Bacon and Carter, 1991), with the waves having been generated by extratropical storms. Recent analyses of the U.S. Atlantic coast buoy data have concluded that the heights of waves generated by hurricanes have on average similarly increased since the 1970s when NOAA buoys became operational (Komar and Allan, 2007a, 2008), as has the seasonal total power generated by the hurricanes (Bromirski and Kossin, 2008). Comparable increases have been found in the Northeast Pacific (waves generated by extratropical storms), documented by measurements from a series of NOAA buoys along the U.S. West Coast (Allan and Komar, 2000; Allan and Komar, 2006; Mendez et al., 2006; Menendez et al., 2008a; Komar et al., 2009), and by analyses of the storm intensities and hindcasts of the generated waves (Graham and Diaz, 2001). While these increases are most likely due to Earth's changing climate, uncertainty remains as to whether they are the product of human-induced greenhouse warming or represent variations related to natural multi-decadal climate cycles. Whatever the cause, the increases are important in their impacts ranging from ship safety to enhanced coastal hazards, and in the engineering design of ocean and coastal structures.

The objective of our study is to examine in detail the progressive increase in wave heights off the coast of the U.S. Pacific Northwest (PNW, Oregon and Washington, Fig. 1), and to examine the range of methodologies available for incorporating that increase into the extreme value assessments employed in engineering and coastal hazard applications. In Allan and Komar (2000, 2006) the analyses focused on the decadal increases in the measured winter significant wave heights (SWHs), including averages of the annual five highest storm-wave occurrences and the maximum annual SWHs. This

* Corresponding author. Tel.: +1 541 737 1239; fax: +1 541 737 1200.
E-mail addresses: ruggierp@geo.oregonstate.edu (P. Ruggiero), pkomar@coas.oregonstate.edu (P.D. Komar), jonathan.allan@dogami.state.or.us (J.C. Allan).

0378-3839/$ – see front matter © 2009 Elsevier B.V. All rights reserved.
doi:10.1016/j.coastaleng.2009.12.005

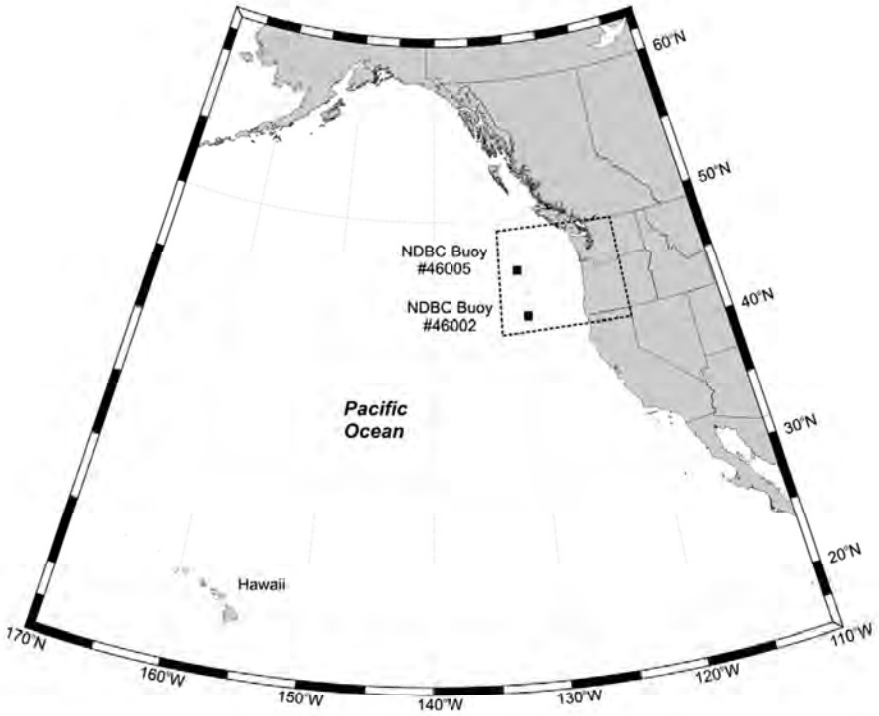

Fig. 1. Map of the west coast of North America with the locations of NDBC buoy #s 46005 and 46002. The black trapezoid indicates the coastal U.S. Pacific Northwest, the states of Oregon and Washington.

increase is further documented here through analyses of the changing probability distributions (histograms) of the complete range of SWHs measured hourly since the buoys became operational in the 1970s. We also examine the sensitivity of the inferred trends to the numbers of quality data included in the regressions, thereby testing the robustness of previously reported long-term trends. The analyses then extend to determinations of the extreme values. After reviewing the conventional time-independent (stationary) approaches, we apply time-dependent extreme value models that have been formulated to deal with non-stationary data such as the wave climate off the PNW coast (e.g., Katz et al., 2002; Stefanakos and Athanassoulis, 2006; Mendez et al., 2006; Menendez et al., 2008a). Finally, we explore how the results of those advanced models depend on their underlying assumptions and the subset of storm-wave data included in the analysis, and how their projections compare with the linear regressions and shifts in the histograms of the full ranges of measured SWHs.

The results of this study are being used in our analyses of coastal hazards along the shores of the U.S. Pacific Northwest. However, beyond that immediate application, the conclusions arrived at in this study concerning the analysis methodologies also have relevance to changes in wave climates identified in the North Atlantic, and potentially elsewhere, where increases in measured SWHs have similarly led to increased extreme value assessments used in applications (Komar et al., 2009).

2. The Pacific Northwest wave climate

The wave climate of the PNW is recognized for its severity, with winter storms commonly generating deep-water SWHs greater than 10 m (approximately one event of this magnitude per year), with the strongest storms in the region having generated SWHs in the range of 14 to 15 m (Allan and Komar, 2002, 2006). The severity of the waves at the latitudes of the PNW (and British Columbia) is the result of the dominant tracks of extratropical winter storms that cross the northeast Pacific (e.g., Change and Fu, 2002).

Of primary interest in the West Coast wave climates analyzed by Allan and Komar (2000, 2006) are the progressive multi-decadal increases in winter SWHs, 'winter' being taken as the months of October through April, the dominant season of strongest storms. The highest rate of increase in wave heights was identified offshore from the Washington coast, with slightly lower rates of increase offshore from Oregon. Northern to central California is a zone of transition having still lower rates of SWH increases, while SWHs off south-central California (Point Arguello) were found to have experienced little net change, the waves there instead being dominated by the inter-annual climate variability associated with the ENSO cycles of El Niños and La Niñas (Allan and Komar, 2006; Adams et al., 2008).

The increase in SWHs off the PNW has been documented primarily with data from National Data Buoy Center (NDBC) (2008) buoy #46005 (and to some extent NDBC buoy #46002 offshore from Oregon), located about 400 km west of the mouth of the Columbia River, a buoy that became operational in the mid-1970s (Fig. 1). Wave data are available from buoys located closer to the coast, over the continental shelf, but their records began in the mid-1980s and suffer from more frequent gaps of missing data, so determinations of long-term trends are more uncertain. Reviews of the NDBC program of wave measurements and analysis procedures can be found in Allan and Komar (2006) and Komar et al. (2009). Of importance, the NDBC operations have been consistent over the decades, and what changes have occurred did not alter the measured SWHs to a degree that would affect the ranges that constitute the wave climate.

The NDBC hourly wave height records have been downloaded from the historical data archives available at the NDBC website (http://www.ndbc.noaa.gov/; accessed June 1, 2008) and analyzed from the beginning of the record (1976 for NDBC buoy 46005) until the end of 2007 (Fig. 2a). The long-term mean SWH at this location is 2.8 m, with the largest SWH measured by the buoy having been 13.6 m, recorded on 1 December 1987. The time series of monthly mean SWHs is presented in Fig. 2b, revealing the distinct seasonality of the PNW wave climate. Monthly mean SWHs are highest in December and January, being 3.9 and 3.7 m respectively. July and August are the calmest months of the year, with monthly mean SWHs averaging 1.6 and 1.7 m respectively.

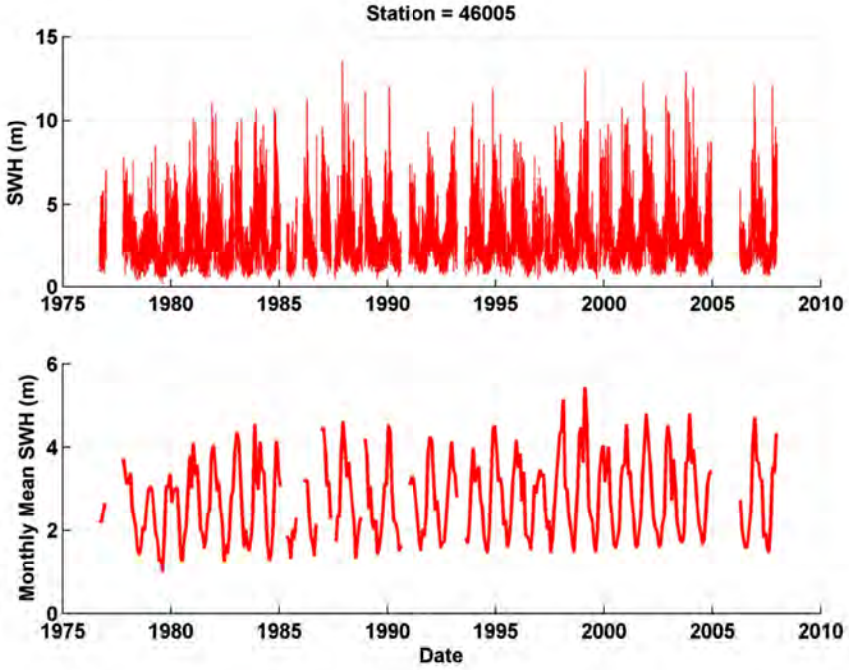

Fig. 2. Time series of a) hourly SWHs and b) monthly mean SWHs for NDBC wave buoy #46005.

The most intense month in the wave record, in terms of monthly mean values, was February 1999 with a 5.4 m monthly mean, the result of four major storms systems that contributed to significant erosion along PNW beaches (Allan and Komar, 2002). The seasonality of the largest storm-wave heights in the region is more fully documented in Fig. 3, with the majority of extreme storms, defined here as exceeding a threshold value of 8.1 m (the 99.5th percentile of the empirical cumulative distribution function), occurring during the winter months. Only five storms classified as extreme, fewer than 4% of the 142 total number of extreme storms, occurred during the calmer 'summer' period between May and September (Fig. 3a).

In our analyses of the NDBC wave data we followed the procedures described by Mendez et al. (2006, 2008) such as having omitted monthly mean SWHs (Fig. 2) for months in which less than 40% of the possible data exists. For extracting annual maxima (Fig. 3b, open circles) from the complete time series, we omitted from the analysis all years in which any month from that particular year's winter season had less than 40% of the possible data. This criterion also follows that

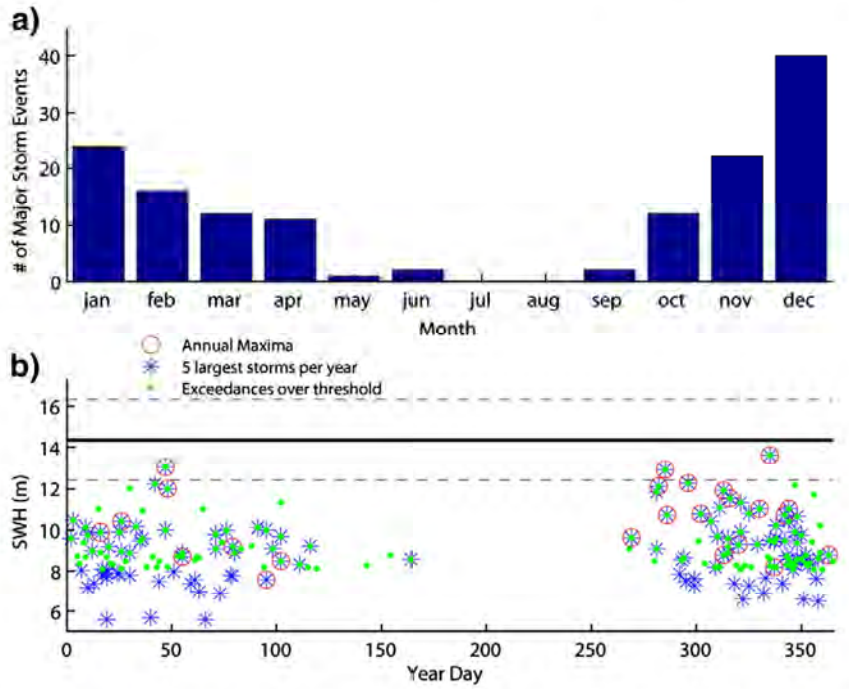

Fig. 3. a) Number of storm events in which the SWH exceeded a threshold of 8.1 m per calendar month. b) Year day of exceedances above the threshold (dots), annual maxima (circles) and the five largest storms per year (asterisks), illustrating the seasonality of the extreme wave climate of the PNW. Also shown is the 100-year SWH return level (solid horizontal line, computed using the AMM approach) and its associated uncertainty (dashed horizontal lines) computed using the delta method (Coles, 2001).

of Gower (2002), but is less stringent than the criteria used by Allan and Komar (2006), which required that 80% of the winter season's data are available for inclusion in the regressions of the annual averages. Later we will discuss the influence of these various criteria on the analyzed trends. For analyses that require extracting multiple extreme storms within a particular year (Fig. 3b, the five largest storms per year are shown as asterisks and exceedances above the threshold are shown as dots), care must be taken to ensure that the individual storms analyzed are independent. Accordingly, the SWH time series has been filtered to eliminate all but the largest reported wave heights within a 72-hour period, a time scale longer than the typical duration of extreme PNW storms.

3. Least squares regressions of annual averages

Assessments of the decadal increases in wave heights for NDBC buoy #46005 are graphed in Fig. 4, similar to the analyses by Allan and Komar (2006) except that here they are extended to include an additional five years of data through the year 2007 and we have used the less restrictive criterion for data inclusion discussed above. Included are the annual averages for the entire year of hourly-measured SWHs, the average winter SWHs, averages of the five largest SWHs recorded each year, and the annual maximum measured SWHs. The rates of increase derived from linear least squares (LLS) regressions are listed on the figure, together with the uncertainties in the regression slopes; each regression is statistically significant at the 95% confidence level. The rate of increase for the annual averages (0.015 m/yr) is comparable to that (0.022 m/yr) found by Bacon and Carter (1991) for the North Atlantic waves measured off the southwest coast of England, suggesting the possibility of their having similar climate controls. While the rate of increase for the annual maximum SWH is slightly lower than reported by Allan and Komar (2006), 0.095 versus 0.108 m/yr, the inclusion of more data has resulted in a statistically significant linear regression rate (at the 95% confidence level) for the annual maximum wave heights.

Although buoy #46005 was selected because it has the least amount of missing data of the deep-water PNW buoys, several 'data gaps' are apparent in Fig. 4 for years when our criterion for data inclusion was not met. The averages for those gaps are shown as open symbols (Fig. 4), but have not been included in the regressions. The most significant gaps occur during the years from 1985 through 1990, the earliest years of 1976 and 1977, and 2005 when the buoy was out of commission for an entire year. The locations of the open symbols indicate that their inclusion would have been in line with the linear regressions, reinforcing the statistical significance of those regressions. The meaningfulness of these long-term trends is also enhanced by Allan and Komar (2000, 2006) having demonstrated that part of the variance not explained by the linear regressions can be accounted for by the range of climate events from El Niños to La Niñas.

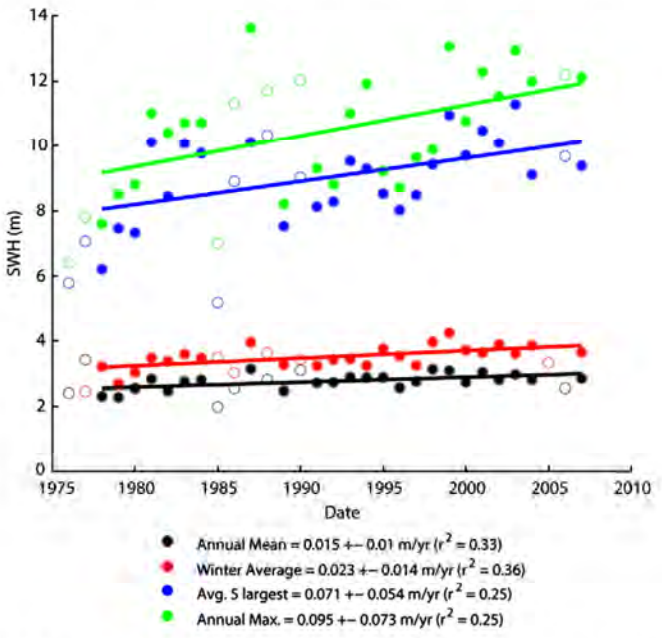

Fig. 4. Decadal increases in annual mean, winter average, average of the five largest per year, and annual maxima SWHs measured by NDBC buoy #46005. The regression slopes and their ± uncertainties are given along with the r^2 values. Each of the regressions is statistically significant at the 95% confidence level. Open circles represent years that did not satisfy the criterion for inclusion and have not been included in the regressions.

Of particular interest in Fig. 4 is the systematic progression of higher rates of increasing wave heights when more extreme assessments are made. By limiting the analysis to winter waves, the rate of increasing wave heights is greater by over 50% compared to the rate for the annual averages (0.023 m/yr versus 0.015 m/yr). Restricting the averages to the five highest measured SWH occurrences each year more than doubles the rate of increase to 0.071 m/yr. The complete list of linear regressions is given in Table 1, including that for the averages of the three highest SWHs, the rate being 0.081 m/yr, above that for the five highest measured SWHs and below the 0.095 m/yr rate for the annual maxima. Included in Table 1 is a column that gives the ratio of the rate of increase for that assessment to the annual average rate of increase (based on the slopes of the linear regressions), further emphasizing this orderly progression. For example, the rate of increase of the annual five largest SWHs is 4.7 times as great as the annual average, while the maximum measured wave heights have increased at a rate that is 6.3 times as great. It will be demonstrated in the following section that this systematic pattern is a reflection of the time evolution of the SWH histograms based on all hourly measurements, with the histograms having probability distributions well described by the lognormal probability distribution function.

To determine the relative robustness of the above regression results, we tested the sensitivity of the computed trends to the amount of data included in the analyses. We first computed regressions using data from the buoy's inception in 1976 through to the year 2000, and then add data from subsequent years until 2007, repeating the analysis for each added year. As shown in Fig. 5, the rates of increase are relatively stable regardless of the amount of data used. The rate of increase in the annual mean SWH and the winter-averaged SWH changes very little with additional data, the range of rates respectively being approximately 20% and 15% of the mean rates. The rate of increase of the average of the 5 largest storms per year and the annual maxima vary by as much as 40% and 30% respectively. Much of this variability is the result of adding data from 2001, 2002, and 2003, years that raised the rate of increase for both the annual maxima and the average of the five largest events per year. Since 2003 the rate of increase of the annual maxima has leveled off, while the rate of increase for the averages of the five largest storms per year has decreased. While the slight differences between the rates of SWH increase reported in Table 1 and those reported by Allan and Komar

Table 1
Rates of increasing SWHs recorded by NDBC buoy #46005 off the PNW coast [modified from Allan and Komar (2006) with the addition of 4 years of data].

Wave height statistic	Rate (m/yr)	25-yr increase (m)	50-yr increase (m)	Ratio to annual average
Annual average	0.015[a]	0.38	0.75	1.0
Average winter	0.023[a]	0.56	1.15	1.5
Five largest	0.071[a]	1.78	3.55	4.7
Three largest	0.081[a]	2.0	4.05	5.4
Annual maximum	0.095[a]	2.4	4.75	6.3

[a] Linear regression is statistically significant at the 95% confidence level including data through the year 2007.

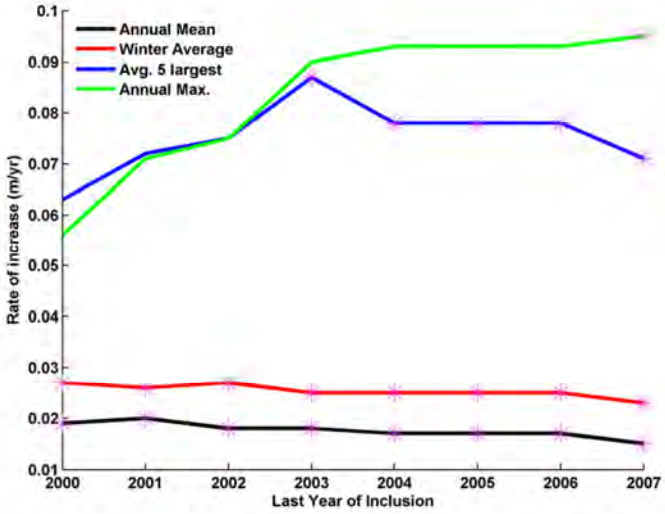

Fig. 5. Rate of increase of the annual mean, winter average, average of the 5-largest, and annual maxima SWHs including data from the inception of buoy #46005 (1976) through to the years 2000 to 2007. The asterisks indicate when the linear regressions are statistically significant at the 95% confidence level.

(2006) are due both to the additional five years of data and the modification of the criterion for data inclusion, the fact that an increase has occurred is a robust result.

The asterisks in Fig. 5 signify that the rates of SWH increases derived from LLS regressions are statistically significant at the 95% confidence level. Note that only when having included data through 2007 does the rate of increase in the annual maxima become significant, explaining the result of Allan and Komar (2006) who found that this regression up through 2002 was not statistically significant. The difficulty in extracting a significant rate of increase for the annual maxima is likely due to the fact that extreme values are not normally distributed, so an LLS regression analysis is not necessarily a reliable method for identifying the long-term trends in extreme waves (Zhang et al., 2004).

4. Decadal shift in wave-height histograms

While Figs. 4 and 5 document the progressive increases in annual averages of the SWHs, a more complete depiction of the PNW wave climate is provided by the probability distributions of all of the hourly measurements. Fig. 6a presents a pair of 'decadal scale' probability distributions for the waves measured by buoy #46005, respectively for the 1976–1990 'decade' immediately following the buoy's deployment, and for the recent decade 1998–2007. While there are clear differences between these two probability distributions (Fig. 6a) in the SWH range between approximately 1 and 8 m, nothing can be deduced about the more extreme wave heights with this conventional approach, even though these extreme waves are most important to coastal erosion impacts and in the engineering design of ocean structures. Therefore, in Fig. 6b the actual numbers of observations are plotted on a log scale to emphasize the extreme but rare occurrences (Komar and Allan, 2007b; Komar et al., 2009). In this way the measured numbers of SWHs greater than 10 m are readily apparent, even though there are only approximately ten occurrences of extreme storms resulting in such large wave heights per decade. The largest measured SWH during each decade plots as 10^0, or 1 occurrence. Note that the 1976–1990 histogram is based on 74,218 hourly-measured SWHs, while the 1998–2007 decade includes 73,671 observations, so that the higher numbers of occurrences of extreme waves in the histogram (Fig. 6b) for the recent decade cannot be attributed to having analyzed more data. Also, the same percentage of data from each decade is from the winter months (approximately 47%), so there is also no seasonal bias between the two individual time series.

Taken together, the pair of standard probability distributions in Fig. 6a and the pair of histograms in Fig. 6b show that the overall range of measured SWHs has shifted toward higher values between the former (1976–1990) and the latter (1998–2007) decades. This increase includes the left limb of the histograms (the lowest measured SWHs), suggesting that there has been an increase in the small waves of the summer as well as in the largest winter waves. This increase is confirmed in Fig. 7, where we have graphed the annual averages of the summer waves, May through September. The LLS regression yields a rate of increase of 0.009 m/yr, small but statistically significant at the 95% confidence level, and consistent with the other regressions (Fig. 4, and Table 1) and with the overall decadal shift in the histograms (Fig. 6).

Fig. 6c depicts the empirical cumulative distribution functions (ECDF) for the two separate decades. The ECDFs illustrate that the 0.005, the 0.5 (median), and the 0.995 quantiles have each shifted to higher values between the two decades, increases of approximately 50% (0.54 to 0.86 m), 10% (2.29 to 2.50 m), and 5% (8.17 to 8.7 m) respectively. These results confirm the regressions in Fig. 4 and Table 1, again demonstrating that the entire wave climate has systematically shifted toward higher values. This finding is developed in greater detail in Fig. 8 by graphing the annual rate of increase of SWHs versus the full range of exceedance percentiles. LLS rates were computed directly from the observed wave data after having derived the empirical SWH probability of exceedance distributions for the years between 1976 and 2007 that pass our data inclusion criteria, this yielding the dashed red curve in Fig. 8. The result is a remarkably continuous increase in the rate of SWH increase towards the tail of the cumulative exceedance distribution.

The pattern evident in the empirically derived curve in Fig. 8 can be explained by analyses of synthetic lognormal SWH climates. While it is well known that the individual waves that make up a narrow banded sea state are Rayleigh distributed (Longuet-Higgins, 1952), there is not a theoretical basis to support the choice of any particular model describing the probability distribution for a long-term (annual to decadal) wave climate (e.g., Ferreira and Guedes Soares, 1999). The lognormal (Jaspers, 1956), Weibull (Battjes, 1972), Generalized Gamma (Ochi, 1992), and Beta (Ferreira and Guedes Soares, 1999) probability distribution functions have each been proposed for modeling SWH climates, but statistical tests to distinguish between the quality of fit for these competing distributions are typically not robust (Guedes Soares, 2003). In Fig. 6a the probability distributions of the two observed decadal SWH climates are shown to be well described by best fit lognormal distributions (thin dashed lines, $R^2>0.97$), the parameters of the theoretical distributions having been fitted to the data via maximum likelihood methods. The fitted lognormal distribution for the second 'decade' shows an increase in large wave heights relative to the fitted distribution of the first decade, corresponding closely to the observations.

The close correspondence between theoretical lognormal distributions and the PNW wave-climate data is the basis for the generation of the solid blue curve in Fig. 8. The initial synthetic SWH climate probability distribution used to create this curve was generated by fitting the scale parameter of a lognormal distribution to the observed SWH time series in 1976. Subsequent synthetic annual lognormal distributed SWH climates, 1977 to 2007, were generated by simply increasing the scale parameter at a rate such that the mean of the synthetic distributions increases at the same rate as the mean of the observed annual SWH distributions. The shape parameter of the annual synthetic lognormal SWH climates was held constant at a full record length best fit value of 0.49 (results are fairly insensitive to this choice). Similar results have been reproduced by fitting Weibull probability distributions to the observed annual SWH climates (not shown). It is evident in Fig. 8 that there is a close correspondence

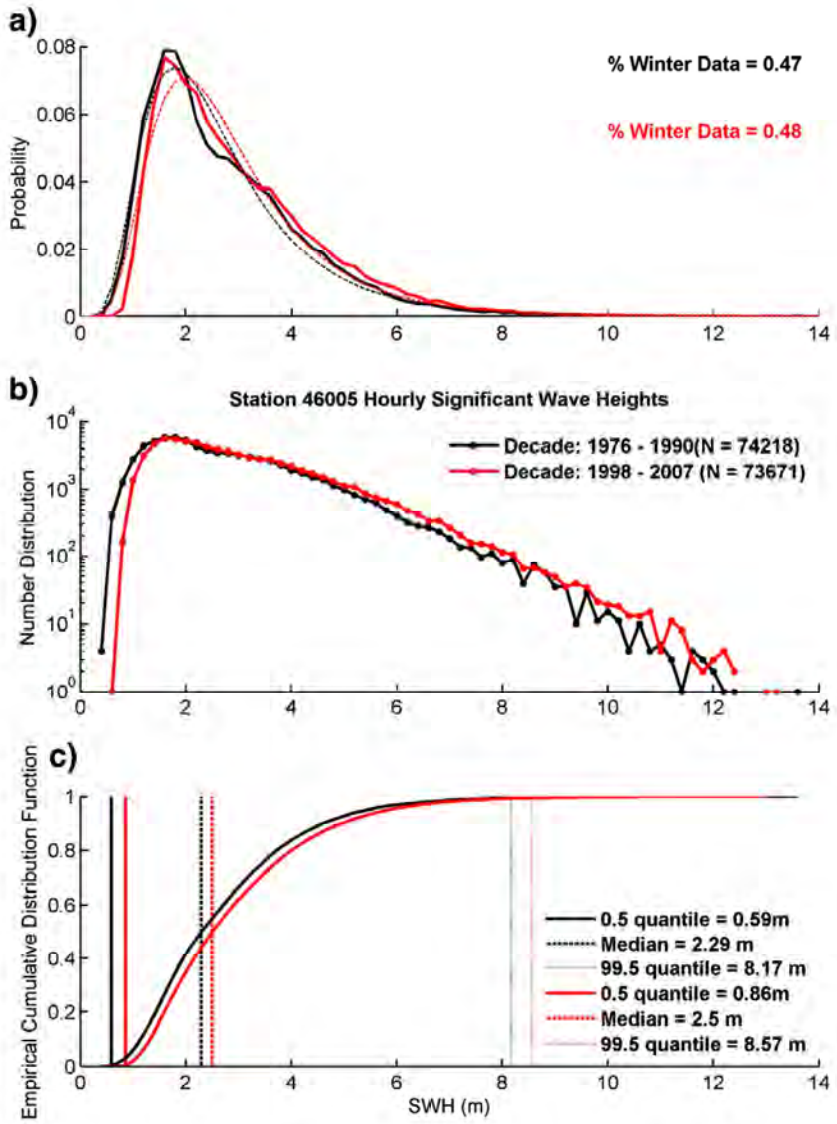

Fig. 6. Comparisons of histograms (probability distributions) for the periods 1976–1990 and 1998–2007, documenting the shift in the wave climate to higher waves. a) Standard probability distribution, b) number distribution plotted on a semi-log scale, and c) empirical cumulative distribution function. The dashed lines in the top panel represent best fit lognormal probability distributions (r^2>0.97).

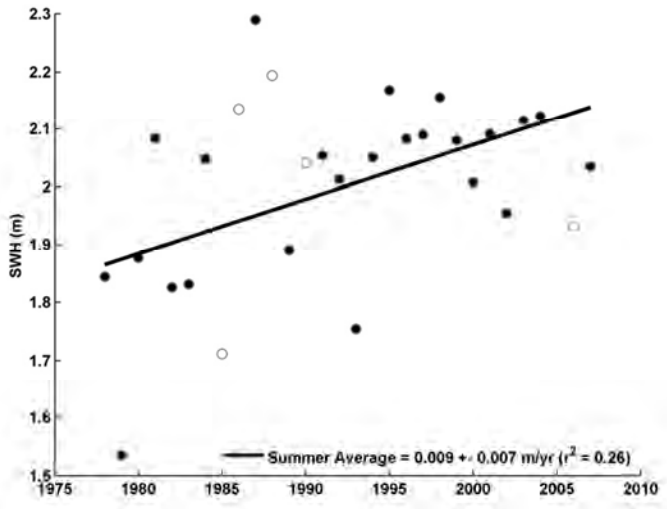

Fig. 7. Decadal increase in 'summer' (May through September) significant wave heights measured by NDBC buoy #46005.

between the annual rates of increasing SWHs based on the theoretical lognormal distribution and the empirical curve derived from the data. Both confirm that for SWH climates, a modest increase in the annual mean can have a significant impact on the frequency and magnitude of extreme events. Therefore, measurements of SWHs off the U.S. PNW coast represent a clear example for a phenomenon that was suggested by Wigley (1988) in general terms; a gradual change in the mean climate of an environmental variable can result in significant increases in the frequency of extreme events.

5. Extreme value assessments

Essential in many applications of wave-climate assessments are projections of the potentially extreme values of ocean wave heights beyond those that have been measured. These applications include the engineering design of ocean structures such as offshore oil platforms and wave-energy extraction units. Predictions of extreme waves are also important in coastal management, to assess flood and erosion hazards faced by coastal populations, infrastructure, and ecosystems. Standard practice has been to apply extreme value statistical models to project the 25- through 100-year SWH return levels generated by

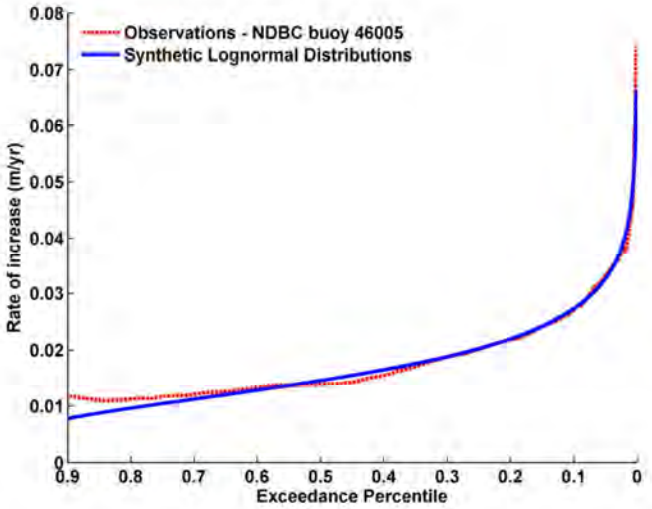

Fig. 8. Rate of increase of annual measured SWH exceedance percentiles for NDBC buoy #46005 (dashed curve) between 1976 and 2007. Rate of increase of annual SWH exceedance percentiles for synthetic lognormal distributions (solid curve) with the scale parameter initialized by a best fit to the 1976 SWH time series and then allowed to increase such that the mean of the synthetic distributions increases at the same rate as that of the observed distributions. The shape parameter of the synthetic lognormal distributions is held constant at a best fit value of 0.49.

major storms, respectively having progressively lower probabilities of occurrence, the 100-year event having a 1% probability during any given year. Those analyses for the most part have assumed that on average the wave data being analyzed are 'stationary', that is, while there generally is a seasonal variation, there has not been long-term trends of progressively increasing or decreasing wave parameters. However, with Earth's changing climate, the corresponding wave climates in many cases have been found to be non-stationary. This is specifically true for the wave buoys along the Oregon and Washington coasts, where both the wave heights and periods have been increasing since the mid-1970s (Allan and Komar, 2000, 2006). The purpose of this section is to examine the applications of various extreme value assessment models to the SWHs measured by buoy #46005, and to compare the projections to the regression trends of the annual averages (Fig. 4 and Table 1) and shifts in the histograms (Fig. 6). The data will first be analyzed applying the conventional extreme value approaches, followed by a series of approaches, in order of increasing complexity, developed to deal with non-stationary data.

5.1. Stationary sequences

In conventional analyses of extreme values, the general assumption is that the wave-height data being analyzed (e.g., the annual maxima) represent independent and identically distributed (stationary) sequences of random variables. The generalized extreme value (GEV) family of distributions is the cornerstone of extreme value theory, in which the cumulative distribution function is given as

$$G(z,\mu,\sigma,\xi) = \exp\left\{-\left[1+\xi\left(\frac{z-\mu}{\sigma}\right)\right]^{-1/\xi}\right\}, \quad (1)$$

defined on $\{z: 1+\xi(z-\mu)/\sigma>0\}$, where the parameters satisfy $-\infty<\mu<\infty$, $\sigma>0$, $-\infty<\xi<\infty$ (Coles, 2001). The model has three parameters; μ is a location parameter, σ is a scale parameter, and ξ is a shape parameter. The EV-II (Frechet) and EV-III (Weibull) classes of extreme value distributions correspond respectively to the cases of $\xi>0$ and $\xi<0$. When $\xi=0$, Eq. (1) collapses to the Gumbel or EV-I type extreme value distribution. By inferring the shape parameter ξ (estimated here, along with the other parameters, by maximizing the log-likelihood function), the data themselves determine the most appropriate type of tail behavior and it is not necessary to make an a priori assumption about which individual extreme family to adopt as in a classical Weibull-type extreme wave-height analysis (Coles, 2001).

The GEV is often applied to annual maxima data in an approach referred to as the annual maximum method (AMM). However, one of the primary shortcomings of fitting an extreme value distribution with annual maximum data is that useful information about the extremes is inherently discarded, particularly when data is sampled on either a daily or hourly basis (as in the case of the SWHs measured by NDBC wave buoys). Two well known approaches exist for characterizing extremes by utilizing data other than simply annual (block) maxima. The first is based on the behavior of the r-largest-order statistics within a block, for low r, and the second is based on exceedances above a high threshold value.

The r-largest-order statistics model yields a likelihood function having parameters that correspond to those of the GEV model for annual maxima, but incorporates more of the observed extreme data (e.g., Coles, 2001; Guedes Soares and Scotto, 2004; Zhang et al., 2004). For the asymptotic arguments of extreme value theory to hold, the number of order statistics r in each year must be chosen carefully. The choice of r is a bias-variance trade off, with small values of r resulting in uncertain parameter estimates and high values of r violating the model assumptions and potentially inducing significant bias. The appropriate choice of r is determined via the likelihood ratio test following the approach of Guedes Soares and Scotto (2004). The likelihood ratio test is based on the deviance statistic, defined as

$$D_{(i,j)} = 2\{\ell_i(M_i)-\ell_j(M_j)\} \quad \text{for} \quad i,j=1,2,\ldots 6 (i\neq j) \quad (2)$$

where $\ell_i(M_i)$ is the log-likelihood function of (M_i). Model (M_j) is rejected relative to model (M_i) at the α level of significance if $D_{ij}>c_\alpha$, where c_α is the $(1-\alpha)$ quantile of the χ^2_1 distribution.

In the peak-over-threshold (POT) method, a high threshold, u, is chosen in which the statistical properties of all exceedances over u and the amounts by which the threshold is exceeded are analyzed. Following Katz et al. (2002) and Mendez et al. (2006), it is assumed that the number of exceedances in a given year follows a Poisson distribution with annual mean νT, where ν is the event rate and $T=1$ year, and that the threshold excesses $y>0$ are modeled using the Generalized Pareto Distribution (GPD) given by

$$H(y,\sigma,\xi) = 1-\left(1+\frac{\xi y}{\sigma}\right)^{-1/\xi} \quad (3)$$

where ξ is the shape parameter of the GEV distribution and σ is a scale parameter related to GEV parameters by $\sigma=\sigma+\xi(u-\mu)$. The event rate can also be expressed in a form compatible with the GEV distribution provided that $\nu=(1+\xi(u-\mu)/\sigma)^{-1/\xi}$.

For each of the three methods discussed above, estimates of extreme quantiles of the distributions are obtained by inverting the distributions in Eqs. (1) and (3). For GEV (and r-largest) analyses the return level, z_p, associated with a return period 1/p is given as

$$z_p = \mu-\frac{\sigma}{\xi}[1-\{-\log(1-p)\}^{-\xi}] \quad (4)$$

and for GPD–Poisson analyses the N-year return level, y_N, is given as

$$y_N = \mu+\frac{\sigma}{\xi}[(Nn_y\zeta_u)^{\xi}-1] \quad (5)$$

where n_y is the number of observations per year and ζ_u is the probability of an individual observation exceeding the threshold u.

Results from applications of each of the three primary approaches to extreme value theory are presented in Fig. 9 for buoy #46005 data, in which we use the entire buoy record length to create return period plots extending to the 100-year event. As with the LLS regression through the annual maxima (Fig. 4), considering the buoy time series from 1976 to 2007 only 24 data points out of a possible 32 are available for an annual maximum method (AMM) GEV analysis. For the GEV analysis the 25-, 50-, and 100-year return levels are respectively 13.2, 13.6, and 13.9 m. For buoy #46005 the most appropriate *r*-largest-order statistic model has an *r* value of 5, resulting in 120 individual storms over the 24 good years of data (the asterisks in Fig. 3b) used for the *r*-largest extreme value analysis. In the POT method the choice of threshold value is also a bias versus variance tradeoff (Mendez et al., 2006). Here we have set the threshold equal to the 99.5th percentile (~8.1 m resulting in 142 individual storms, approximately 5.2 storms per year), the threshold that was also employed in the model of Mendez et al. (2006). Later in the paper we will discuss the sensitivity of the results to the value chosen for the threshold. While the POT approach results in the most conservative 25- through 100-year return levels of the three models (Fig. 9c), the return levels derived from the three models are nearly the same, their difference being less than approximately 3%.

Similar to the varying LLS regression results shown in Fig. 5, it is important to understand the influence of including more or less data on the stability of the results for each of the extreme value distributions, to determine their relative robustness (the 32 year record length of buoy #46005 being one of the longest in the NDBC program). In Fig. 10 we again include additional data stepwise from the year 2000 through to 2007, as done in Fig. 5 for the LLS regressions. The 100-year return level SWH (and the other return levels associated with the 25- and 50-year return periods, not shown) is seen to be fairly insensitive to having included additional years, the main change being the reduction in the width of the 95% confidence interval around the return level inferences. Fig. 10b reflects the number of data points used in each of the three analysis techniques as a function of time. The insensitivity of the results to the amount of data included suggests that a fairly robust projection of the 100-year SWH for buoy #46005, using these stationary approaches, is approximately 14.0 ± 2 m at the 95% confidence level (Fig. 10a). This projection is consistent with the highest measured SWH in the buoy's time series, 13.6 m. However, in the next section it will be demonstrated that these extreme value projections are in fact non-conservative due to the non-stationarity of the time series, and therefore are not necessarily appropriate for applications.

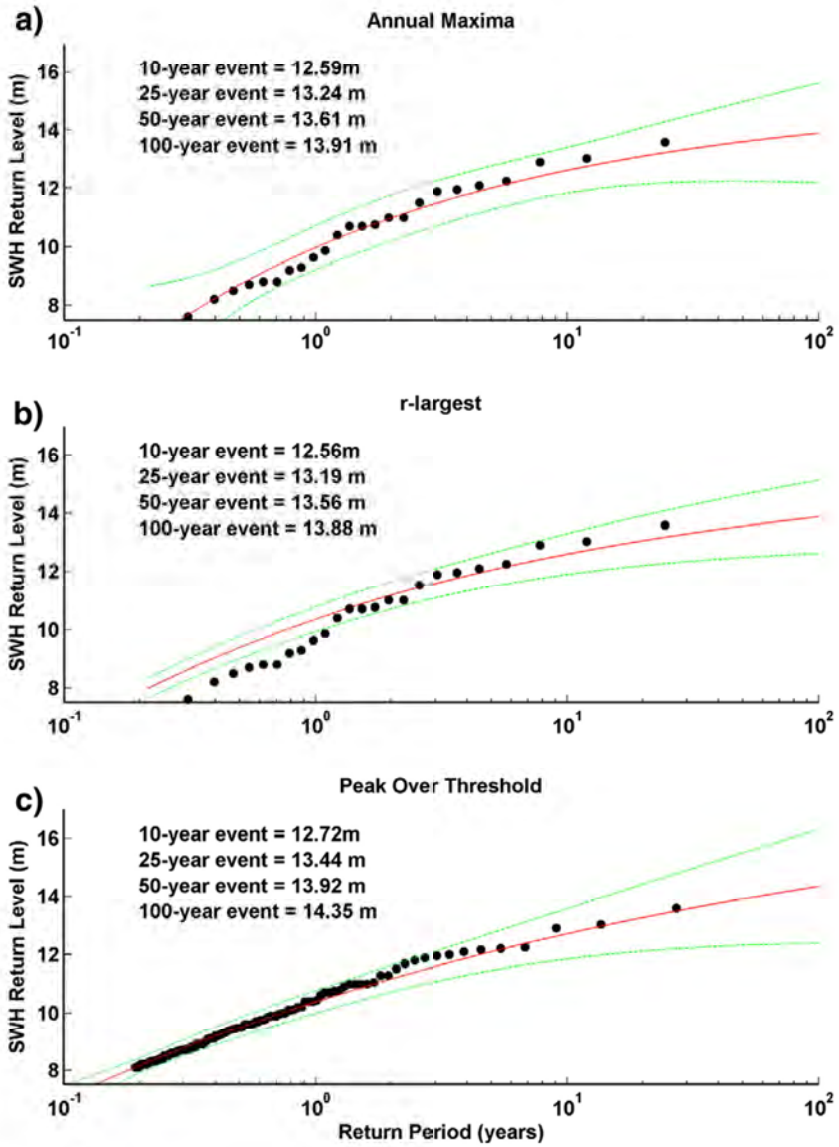

Fig. 9. Extreme SWH return levels calculated via a) annual maxima GEV, b) *r*-largest-order statistics model, and c) peak-over-threshold model for NDBC buoy #46005. Dashed lines represent the 95% confidence intervals on the return levels computed using the delta method (Coles, 2001).

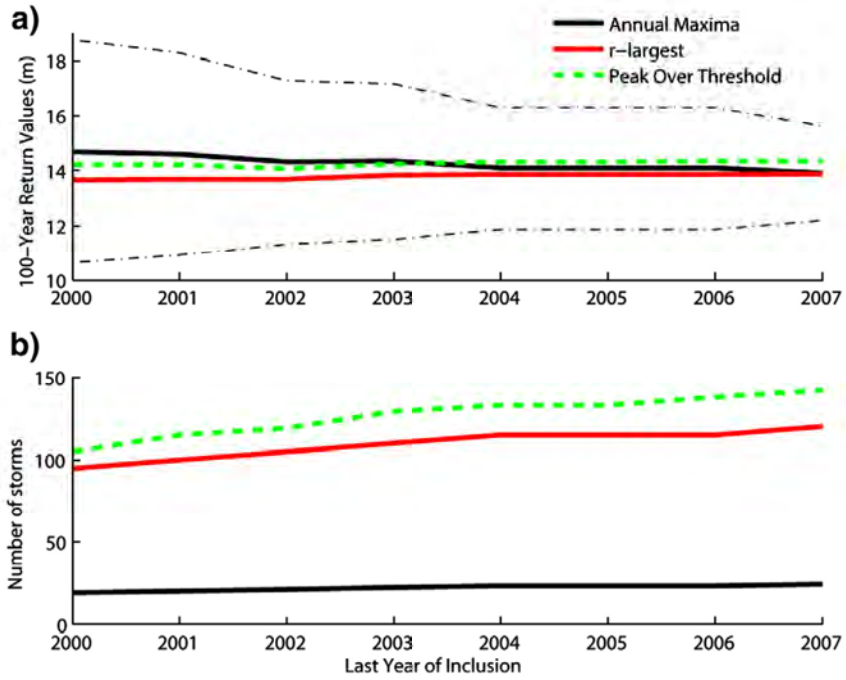

Fig. 10. a) 100-year return levels for NDBC buoy #46005 as a function of the last year of data inclusion for the annual maxima GEV method, the *r*-largest-order statistics model, and the peak-over-threshold model. Dash–dot lines are the 95% confidence intervals on the GEV method as computed using the delta method (Coles, 2001). b) Number of storms included in the extreme value analyses as a function of the last year of data inclusion.

5.2. Non-stationary sequences

With global climate change and variability the assumption of a stationary wave climate is no longer valid in many situations, as trends of increasing SWHs have clearly been documented in both the North Atlantic and Northeast Pacific. Projections of the extreme values used in applications must therefore take into account trends and variability in the measured waves, and to the extent possible acquire an understanding of their underlying climate controls (Komar et al., 2009). A variety of procedures have been developed to undertake extreme value assessments for time-varying data populations, directed in many cases toward environmental changes that are a result of global warming, such as increased rainfalls and river discharges (e.g., Katz et al., 2002). These approaches range from simply extrapolating extreme value projections using trends derived from the historical record, to fitting separate extreme value distributions to different periods within the data record (Zwiers and Kharin, 1998), and in the most sophisticated analyses applying statistical models such as those of Zhang et al. (2004) and Mendez et al. (2006, 2008) that directly incorporate non-stationary processes in assessments of extreme values. Here we examine this range of procedures, in order of increasing complexity, directed toward assessments of the extreme wave climate of the PNW.

The systematic increase in annual averages of the highest measured SWHs, Fig. 4 and Table 1, supports a level of confidence in accepting a projected rate of increase of the largest wave height per year that is on the order of 0.095 m/yr. With that rate of increase for the annual maxima, the 25-year SWH (based on the AMM, Fig. 9a) can be extrapolated to increase by approximately 2.4 m over the next 25 years, reaching a SWH of 15.6 m. By 2032 (25 years after the last data analyzed) the 50- and 100-year return levels would respectively be 16.0 m and 16.3 m if the rate of increase maintains that high rate, an uncertain assumption considering that there is only a 32-year measurement record. On the other hand, the projections might be reasonable in that SWHs of 14 to 15 m have actually been measured by NDBC buoys off the PNW coast, during the March 1999 (Allan and Komar, 2002) and December 2007 storms, by the inshore buoys over the continental shelf where the storms had intensified.

Another simple approach for deriving time-varying extreme value projections is to base them on distinctly different periods of measured SWHs, such as shown in the decadal histograms of Fig. 6. This approach considers the individual histograms as representing quasi-static wave climates and uses conventional extreme value models to project the 25- to 100-year extreme SWHs for each subset of the data. Accordingly, the annual maximum measurements for the 1976–1990 and 1998–2007 decades analyzed in Fig. 6 respectively yield 13.6 and 13.24 m for the 25-year projections, and 14.6 and 13.32 m for the 50-year extremes (via an AMM GEV analysis). These values are clearly unreasonable since the highest measured SWH occurred during the first decade analyzed, and therefore the higher extreme values are projected from the first subset of data, in direct contrast to the results from the linear regressions (Fig. 4). Furthermore, only a few data points are available for each decade (~10), so the results have large error bars. Based on this example, we conclude that this approach generally will not yield reasonable results for projections of the rates of increase of extreme design waves into the future.

A more pragmatic approach to analyzing the extremes of non-stationary environmental data can be applied to each of the three types of extreme value analyses described above (AMM, *r*-largest, and POT). These advanced statistical procedures involve a direct extension of the conventional extreme value analyses, an extension that does not assume the wave climate has remained stationary over the decades, thereby being able to account for progressive changes in the extreme value assessments (Coles, 2001; Katz et al., 2002; Zhang et al., 2004; Mendez et al., 2006; Eastoe and Tawn, 2008). For example, variations in the observed process can be modeled as a time-dependent trend in the location and scale parameter of the GEV distribution, such that

$$\mu(t) = \mu_0 + \mu_1 t, \quad \log\sigma(t) = \sigma_0 + \sigma_1 t, \quad \xi(t) = \xi \tag{6}$$

In this case the parameter μ_1 corresponds to the annual rate of change in the location parameter, such that the time-homogenous model (Eq. (1)) forms a special case of the time-dependent model, with $\mu_1 = 0$ and $\mu = \mu_0$ (Coles, 2001). While in Eq. (6) the location

parameter is modeled as a linear function of time, it could instead be modeled as varying with time either exponentially or quadratically. Due to the difficulty in estimating the shape parameter with precision, it is typically not modeled as a function of time (Coles, 2001). In the time-dependent GPD–Poisson model the event rate is also a function of time since it is related to the modeled time-dependent parameters.

The results of such an application to buoy #46005 are given in Fig. 11, with the data analyzed again being the annual maxima (AMM approach), the five largest SWHs measured each year (*r*-largest), and the exceedances over the 99.5th percentile of the time series (POT). The three solid lines included in Fig. 11 are the time-dependent 100-year SWH return level projections, each increasing at a rate determined by the non-stationary extreme value analyses. Time is linearly modeled as a covariate via the location parameter in each of the three models.

All of the trend rates found in these analysis results (Fig. 11) are statistically significant at the 95% confidence interval. Significance is determined when the deviance statistic (Eq. (2)), computed for a model including the trend and for a model without the trend, is large relative to the χ^2_1 distribution implying that the trend explains a substantial amount of the variance in the data. Modeling time as varying exponentially via the location parameter, as was done by Mendez et al. (2006), also results in statistically significant trends (not shown) that are slightly smaller than the trends derived from the linear covariate models for each of the three approaches. However, the time-dependent linear models and time-dependent exponential models are not significantly different, via the deviance statistic, and therefore choosing the exponential models over the linear models is not justified. Similarly, for each of the three classes of extreme value theory the inclusion of time dependence in the scale parameter results in models that are not significantly different from models with time dependence in the location parameter alone. This is a similar result to that found by Mendez et al. (2006), and therefore, following the principal of parsimony, we report on cases where only the location parameter is modeled as a linear function of time (Fig. 11). We note, however, that Menendez et al. (2008b) have reported on wave-height data from other locations in which time dependence in both the location and scale parameters are statistically significant.

The dashed lines in Fig. 11 represent the LLS regression trend lines through the data themselves. For both the time-dependent AMM and *r*-largest approach, the trends derived from extreme value theory yield results that are very close to those from the LLS regressions. Only the trend derived from the time-dependent POT method is significantly greater than the linear regression through the data that exceeds the 8.1-m threshold, a point we will discuss in detail later.

The 100-year return level in 2032 derived from the non-stationary AMM model is approximately 18.5 m (Fig. 11 and Table 2), significantly higher than the 100-year return level derived from the stationary approach, 13.9 m (dashed–dot line in Fig. 11). This projected non-stationary extreme value is also higher than the result from the simple approach discussed above, in which the stationary return level is simply extrapolated to a time-dependent value at 2032 using the results of the LLS analyses (Fig. 11). The non-stationary *r*-largest and POT approaches yield 100-year return values for year 2032 that are also higher than simply extrapolating the stationary return level by the LLS trend rate (the closed diamonds in Fig. 11).

While the 100-year return values were shown to be relatively independent of the technique when using time-independent extreme value theory (Figs. 9 and 10), in contrast there is significantly more separation in the 100-year return values computed with time-dependent extreme value theory, projected 25 years beyond the last data included in the analysis. As expected, the differences in the 2032 100-year event (a wave height projected to have a 1% chance of occurring in year 2032) vary with the long-term rate of wave-height increase derived from each technique. The POT method gives a 2032 100-year return level of approximately 15.9 m, while the *r*-largest and AMM methods give 16.6 m and 18.5 m respectively (Fig. 11).

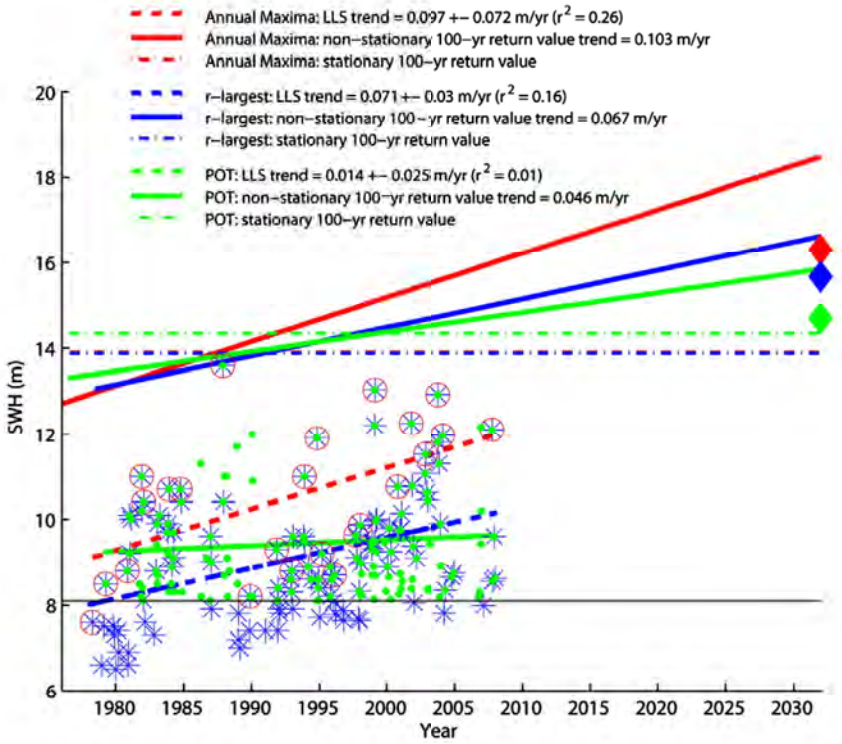

Fig. 11. Data included in GEV analysis of annual maxima (circles), *r*-largest analysis of 5 largest storms per year (asterisks), and POT analysis of storms larger than 8.1 m (dots). The thick dashed lines represent the LLS regression trends through the data while the thick solid lines represent the time-dependent 100-year return periods computed using extreme value theory. The 100-year return periods have been projected out 25 years beyond the last data included in the analysis to the year 2032 (solid lines). Shown for comparison are the stationary 100-year return levels for each of the three classes of extreme value theory (thin dash–dot lines) and the linear extrapolations of these stationary return levels to 2032 using the LLS trends (filled diamonds).

Table 2
Various statistics for NDBC buoy #46005 and NDBC buoy #46002, and the combined time series.

Statistic	NDBC buoy #46005	NDBC buoy #46002	Combined time series #46005 and #46002
0.5th percentile (m)	0.70	0.79	0.70
50th percentile (m)	2.41	2.39	2.40
99.5th percentile (m)	8.09	7.89	8.04
LLS annual mean (m/yr)	0.015[a]	0.01	0.013[a]
LLS summer avg. (m/yr)	0.009[a]	0.007	0.007[a]
LLS winter avg. (m/yr)	0.023[a]	0.016	0.025[a]
LLS POT (99.5%) (m/yr)	0.014	0.005	0.01
LLS 5 largest (m/yr)	0.071[a]	0.037	0.049
LLS annual max. (m/yr)	0.097[a]	0.054	0.07
GEV trend AMM (m/yr)	0.103[b]	0.052[b]	0.07[b]
R-largest trend (m/yr)	0.067[b]	0.053[b]	0.039[b]
POT trend (m/yr)	0.046[b]	0.028[b]	0.036[b]
POT 25-year return level (m)	13.44	13.81	13.4
POT 50-year return level (m)	13.92	14.36	13.9
POT 100-year return level (m)	14.35	14.84	14.35
AMM 100-year return level in 2032 (m)	18.5	14.37	16.69
R-largest 100-year return level in 2032 (m)	16.6	15.08	15.38
POT 100-year return level in 2032 (m)	15.9	15.81	16.27

[a] Linear least squares (LLS) regression is statistically significant at the 95% confidence level including data through the year 2007.
[b] Extreme value theory derived trend is statistically significant at the 95% confidence level.

Projecting further into the future produces a still greater spread in the model results. Of interest the 100-year return levels derived with the three time-independent techniques represent wave heights that are projected to have a 67%, 33%, and 10% chance of occurring in 2032 according to the non-stationary AMM, *r*-largest, and POT models respectively.

Finally, we examine the influence of the threshold selection in the POT approach on both the return levels and the differences between the LLS derived trends and the POT derived trends (Fig. 12). Surprisingly, changes in those trends are inversely correlated (correlation coefficient equal to −0.76) over a range of thresholds from 7 m to 9 m. Fig. 12b illustrates that while increasing the threshold from 7 m to 9 m has little impact on the time-independent 25- through 100-year return levels, the return levels projected for the year 2032 (25 years from the last data included in the analysis) mirror the variability shown in the POT derived long-term rates.

6. Discussion

The results of our above analyses, limited to buoy #46005 seaward of the Columbia River, are reasonably consistent whether they are based on LLS regressions of annual average SWH statistics, histograms of the full range of measured SWHs, or projections of future extreme values including those based on non-stationary methodologies. However, two additional issues remain to be considered, the first involving a test of the consistency of the results in comparison with the other deep-water buoy in the region, and secondly a resolution with the sophisticated models developed by Mendez et al. (2006, 2008) and Menendez et al. (2008a,b) that derived long-term progressive trends of increasing SWHs that are substantially lower than those found in our analyses.

6.1. Application to NDBC buoy #46002

While the results discussed above suggest that the trend of increasing wave heights off the PNW coast is robust, it is of interest to determine if the other deep-water buoy in the region, off the southern Oregon coast, has documented the same phenomena and yields similar results in terms of the extreme value projections. Buoy #46002 is located about 450 km west of Coos Bay, OR in approximately 3500 m of water (Fig. 1). The buoy began operation in 1975 but has experienced more gaps of missing data than buoy #46005. While 24 years out of a possible 32 satisfied our 'good data year' criterion for buoy #46005, only 16 years out of 33 possible are considered good data years for buoy #46002 (Fig. 13b). We have completed the same series of

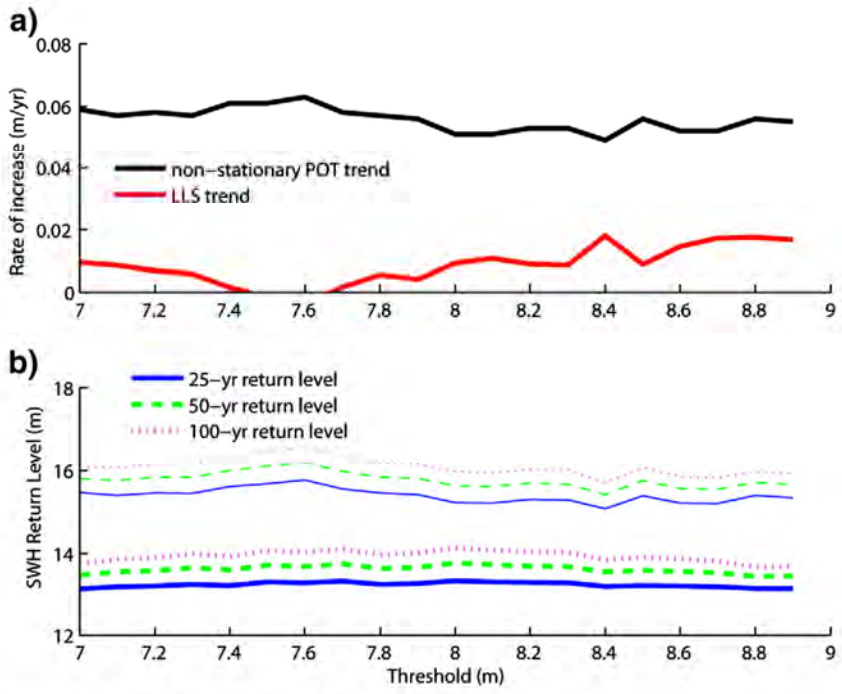

Fig. 12. a) Influence of a variable (stationary) threshold value on the LLS trend derived from the data (above the threshold) and the trend computed directly from the non-stationary POT model. b) Variations in time-independent 25- through 100-year return levels for variable thresholds values included in the POT extreme value approach (thick lines) and variations in the time-dependent POT return levels projected for 2032 (thin lines).

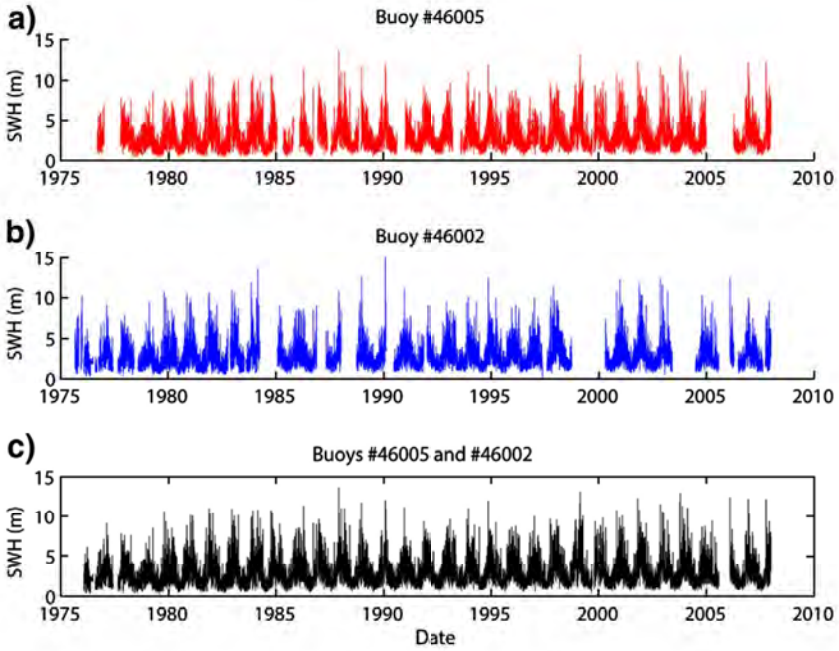

Fig. 13. a) NDBC buoy #46005 time series, b) NDBC buoy #46002 time series, and c) the combined time series constructed using buoy #46002 to fill gaps in the time series of buoy #46005.

analyses for the Oregon buoy as those presented above for the Washington buoy. As found by Allan and Komar (2006), the trends of increasing SWHs for buoy #46002 are slightly lower than those measured by buoy #46005, part of the overall north to south West Coast latitude variation. However, the main implication of the considerable data gaps in the Oregon buoy data is that some of the LLS trends are not statistically significant (Table 2). The trends of increasing wave heights derived from each of the three time-dependent extreme value theory applications are, however, statistically significant.

Finally, we have developed a combined time series in which we fill the data gaps in buoy #46005 with data from buoy #46002, if it was operational at that time (Fig. 13c). A primary advantage of this combined time series is that now 29 out 32 years achieve our 'good data year' criterion. Once again the trends of increasing wave heights derived from extreme value theory are statistically significant. The 25- through 100-year return levels are also fairly consistent (Table 2), regardless of the methodology and regardless of the time series (buoy #46005, #46002, or the combined time series) used in the analysis.

6.2. Variable thresholds and storm seasonality

Mendez et al. (2006, 2008) and Menendez et al. (2008a,b) have developed advanced extreme value (GPD–Poisson) models to estimate long-term trends in the frequency and intensity (and duration in some cases) of severe storm waves, yielding significant extensions to the simple time-dependent version of the POT approach we have applied here. As presented in the most advanced stage of development, their models can account for the seasonal variability of SWHs above a constant threshold value, and are capable of including dependencies on various climate indices. Of interest here is that the models described in Mendez et al. (2006) and Menendez et al. (2008a) were also applied to buoy #46005 off the coast of the PNW; however, they reported substantially lower trends for the long-term progressive increase in extreme SWHs than the rates found by Allan and Komar (2002, 2006) and in our results presented above.

The model by Mendez et al. (2006) that yielded the best overall assessment of the multitude of variations in the SWHs above an 8.1-m threshold produced a net rate of annual increase of only 0.032 m/yr (0.035 m/yr without a dependence on climate indices). We note that this rate of increase is associated with the 94.2th percentile of the empirical cumulative distribution function of all hourly SWH measurements from buoy #46005 (Fig. 8), a percentile in turn associated with a long-term average SWH of only 5.2 m. Mendez et al. (2006) argue that the long-term trend derived from their time-dependent POT model is more reliable than the LLS regression trends obtained by Allan and Komar (2000, 2006) and updated here. However, based on the range of methods we have presented in this paper it is not clear that a time-dependent POT approach including seasonality, and computed with a constant threshold value, is the best overall method for determining long-term trends for all applications. In Table 2 we compare long-term trends derived from the three primary time-dependent extreme value theory approaches. Our time-dependent AMM model gives a rate of increase of 0.103 m/yr (again using data through 2007, rather than 2004 as in Mendez et al., 2006), and our r-largest model results in a long-term trend of 0.067 m/yr (using r equal to 5). Our simple time-dependent POT model reveals a rate of increase in wave heights of 0.046 m/yr (modeling wave height as linearly increasing in time via the location parameter, rather than exponentially as in Mendez et al., 2006). As discussed previously, a primary drawback of the AMM approach is that all but one severe wave height per year is ignored, so it is fair to conclude that of the three approaches the AMM is the least robust. However, as r in the r-largest technique increases the number of storms included in the extreme value analysis can approach that included in the POT technique, making it difficult to dismiss results from this approach.

The differences between a long-term trend derived from the r-largest and the POT approaches can be visualized by the data included in Fig. 11. With the POT threshold value set at 8.1 m, several moderate storms that satisfy the criterion to be included in the r-largest method are in fact excluded in the POT approach. Because many of these storms occurred relatively early in the record, the LLS regression through the threshold exceedances gives a fairly small and statistically insignificant rate of increase of 0.014 m/yr. In contrast, the relatively high regression slope of 0.071 m/yr (0.097 m/yr) represents an LLS fit through the 5 largest (annual maximum) storms each year. In this case, analyzing only the data that exceed the constant

threshold misses the increasing storminess that clearly characterizes this data. While the POT approach includes an a priori unlimited number of extreme storms per year that exceed a threshold, it by definition ignores waves below the threshold that may well have been the largest waves that occurred early in the record. It is relatively straightforward to demonstrate that the inclusion of a time-varying threshold value, e.g. varying in magnitude by the long-term trend in the 99.5th percentile, results in a GPD–Poisson model derived long-term rate (assuming a linear trend in the location parameter and not including seasonality) that is approximately 20% higher than the rate determined by the constant threshold approach (respectively 0.055 m/yr and 0.046 m/yr, not shown). Additional problems associated with using constant threshold values for non-stationary data are discussed by Eastoe (2008) and Eastoe and Tawn (2008).

In Fig. 14 we show how the rate of increasing wave heights varies with the number of storms included in the *r*-largest analysis. The long-term trend rate decreases asymptotically from approximately 0.1 m/yr when *r* equals 1 (the AMM method) to approximately 0.065 m/yr for *r* equals 10. The trend rate derived from the non-stationary *r*-largest extreme value approach behaves in a very similar manner to that derived from LLS regression. In contrast, the long-term trend derived from the POT approach has a markedly different behavior than the LLS regressions through the wave heights exceeding a particular threshold (Fig. 12b). The difference in both magnitude and variability of the long-term rates derived by LLS and POT extreme value models with the choice of a constant threshold again suggests that caution should be used when applying rates derived in this manner. Interestingly, the LLS rate derived with storm wave heights above a time-varying threshold (not shown) is approximately the same as that derived from time-dependent extreme value theory (respectively 0.052 m/yr and 0.055 m/yr).

Both Mendez et al. (2008) and Menendez et al. (2008b) point out that the inclusion of seasonality in their time-dependent POT model should lead to improved designs of maritime works where assessments of variations in storm waves throughout the year is important. For example, accounting for this seasonal variability may be important in the design of wave-energy farms, which have been proposed for the PNW coast. However, for applications such as the potential failure of the designed works, or future potential hazards from coastal erosion and flooding, seasonality is of little importance since those extreme hazards are associated with winter storms and the more conservative long-term rates of wave height increases derived without seasonality should also be considered.

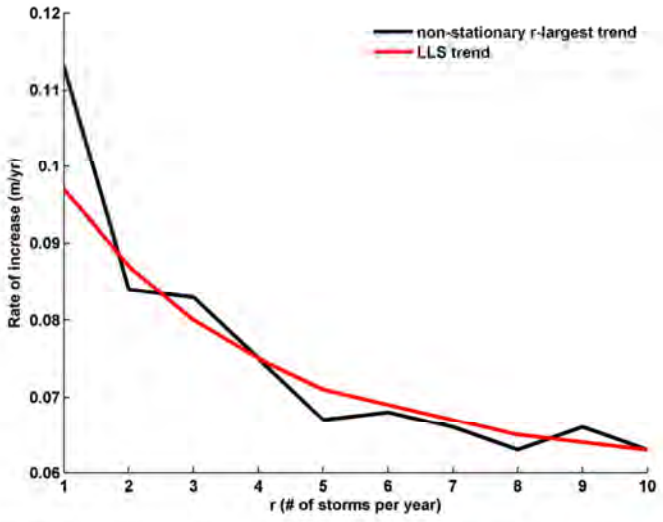

Fig. 14. Long-term trend of increasing SWHs computed via LLS regression analysis and the non-stationary *r*-largest extreme value approach as a function of the number of highest storms per year, *r*, included in the analysis.

7. Summary of conclusions

Increasing storm intensities and the heights of the waves they generate have been documented in both the North Atlantic and North Pacific. Although the climate controls have not been firmly established, the increasing wave heights are clearly important in their impacts ranging from ship safety to enhanced coastal hazards, and in the engineering design of ocean and coastal structures. The objective of this paper has been to further quantify these trends of increasing wave heights and to explore how they can be projected into the future to derive design waves used in applications. The analyses presented here have centered on wave data collected in deep water off the coast of the U.S. Pacific Northwest (Oregon and Washington), mainly by buoy #46005 of NOAA's National Data Buoy Center (NDBC) (2008).

A variety of analyses have been applied to the hourly-measured significant wave heights (SWHs) collected between 1976 and 2007, directed toward assessing the decadal increase and the potential future extremes, including the 25- through 100-year projected SWHs. The simplest approach has been to graph the annually averaged SWHs, with their overall trends being based on linear regressions. The annual averages of the deep-water SWHs have increased at a rate of approximately 0.015 m/yr, while averages for the winter season (October through March) increased at the higher rate of 0.023 m/yr. Of interest in applications are the rates of increase of the highest measured SWHs each year, those generated by major storms. Averages of the five highest SWHs measured each year have increased at the appreciably greater rate of 0.071 m/yr, with the rate for the annual maximum SWHs having been 0.095 m/yr. Analyses were undertaken of the statistical significance of these trends and how they have changed with time by the addition of more data. All of the trends are statistically significant at the 95% confidence level.

Histograms of the hourly-measured SWHs further document this shift toward higher values over the decades. Both the highest waves generated by major storms and the relatively low waves of summer have experienced significant increases. The observation that the more extreme the SWH percentile analyzed the faster the rate of increase is shown to be a fundamental result of the observed wave height probability distributions being well described by lognormal (or Weibull) probability distribution functions.

The non-stationary nature of the PNW wave climate translates into substantial increases in extreme value projections relative to stationary projections. Results for the progressive increases in the 25- to 100-year projections depend somewhat on the assumptions made in the statistical procedures, on decisions as to the numbers of storm-wave heights included, or the threshold value of the measured SWHs for inclusion in the analyses. Of significance, the results from the procedures that model the non-stationarity of the data are typically consistent with the linear regressions of annual averages and the observed shifts in the wave height histograms.

Whichever modeling approach is used, projecting time-dependent extreme values into the future implies that the underlying cause of the long-term trends is understood and that this behavior will continue. However, our knowledge of the detailed climate controls on trends in storminess and their generated waves is still incomplete, with climatologists having attributed the increases in the North Pacific to both global warming in general and to increased particulate pollutants in the atmosphere. Until more is known about how variations in Earth's climate affect the PNW deep-water wave climate, projected extreme values should be considered as uncertain and care should be used when applying these various techniques to real-world coastal engineering and management problems.

Finally, we note that the analyses presented here, based on data from NDBC buoy #46005, some 400 km seaward from the Columbia River (and to some extent buoy #46002 offshore from southern Oregon), were undertaken with the objective of exploring the methodologies directed toward assessments of the extreme value projections where

there are increasing wave heights (and periods). Our research is now directed toward applying these models in the development of complete wave climates for the PNW (the coasts of Washington, Oregon and Northern California), which incorporate wave data from a number of inshore buoys, at intermediate water depths over the continental shelf. In that recent major storms have developed over the shelf and generated some of the most extreme measured SWHs, on the order of 15 m (Allan and Komar, 2002), the formulation of wave climates directed toward applications along the PNW coast clearly need to include those measurements.

Acknowledgements

The authors gratefully acknowledge the support of the Sectoral Applications Research Program (SARP) of the U.S. Department of Commerce's National Oceanic and Atmospheric Administration (NOAA) under NOAA Grant #NA08OAR4310693. Lead author Ruggiero was also supported by NOAA's National Sea Grant College Program under NOAA Grant #NA06OAR4170010 and the Pacific Region Integrated Climatology Information Products (PRICIP) project of the NOAA NCDC Integrated Data and Environmental Applications (IDEA) Center via the East West Center's Grant HC #12255 at the time of writing this paper.

References

Adams, P.N., Inman, D.L., Graham, N.E., 2008. Southern California deep-water wave climate: characterization and application to coastal processes. Journal of Coastal Research 24 (4), 1022–1035.

Allan, J.C., Komar, P.D., 2000. Are ocean wave heights increasing in the eastern North Pacific? EOS. Transaction of the American Geophysical Union 81 (47), 561–567.

Allan, J.C., Komar, P.D., 2002. Extreme storms on the Pacific Northwest Coast during the 1997–98 El Niño and 1998–99 La Niña. Journal of Coastal Research 18, 175–193.

Allan, J.C., Komar, P.D., 2006. Climate controls on U.S. West Coast erosion processes. Journal of Coastal Research 22, 511–529.

Bacon, S., Carter, D.J.T., 1991. Wave climate changes in the North Atlantic and North Sea. International Journal of Climatology 11, 545–558.

Battjes, J.A., 1972. Long term wave height distributions at seven stations around the British Isles. Deutsche Hydrographische Zeitschrift 25, 179–189.

Bromirski, P.D., Kossin, J.P., 2008. Increasing hurricane wave power along the U.S. Atlantic and Gulf coasts. Journal of Geophysical Research 113, C07012. doi:10.1029/2007/JC004706.

Carter, D.J.T., Draper, L., 1988. Has the north-east Atlantic become rougher? Nature 332, 494.

Change, E.K.M., Fu, Y., 2002. Interdecadal variations in Northern Hemisphere winter storm track intensity. Journal of Climate 15, 642–658.

Coles, S.G., 2001. An introduction to statistical modeling of extreme values. London, Springer. 208pp.

Eastoe, E.F., 2008. A hierarchical model for non-stationary multivariate extremes: a case study of surface-level ozone and NOx data in the UK. Environmetrics. doi:10.1002/env.938.

Eastoe, E.F., Tawn, J.A., 2008. Modelling non-stationary extremes with application to surface level ozone. Journal of the Royal Statistical Society 58 (1), 25–45.

Ferreira, J.A., Guedes Soares, C., 1999. Modelling the long-term distribution of significant wave height with the beta and gamma models. Ocean Engineering 26, 713–725.

Gower, J.F.R., 2002. Temperature, wind and wave climatologies, and trends from marine meteorological buoys in the northeast Pacific. Journal of Climate 15, 2709–3717.

Graham, N.E., Diaz, H.F., 2001. Evidence for intensification of North Pacific winter cyclones since 1948. Bulletin of American Meteorological Society 82, 1869–1893.

Guedes Soares, C., 2003. Probabilistic Models of Waves in the Coastal Zone. In: Lakhan, C. (Ed.), Advances in Coastal Modeling. Elsevier Science, pp. 159–187.

Guedes Soares, C., Scotto, M.G., 2004. Application of the r largest-order statistics for long-term predictions of significant wave height. Coastal Engineering 51, 387–394.

Jaspers, N.H., 1956. Statistical distribution patterns of ocean waves and of wave induced stresses and motions with engineering applications. Transactions Society Naval Architects and Marine Engineers 64, 375–432.

Katz, R.W., Parlange, M.B., Naveau, P., 2002. Statistics of extremes in hydrology. Advances in Water Resources 25, 1287–1304.

Komar, P.D., Allan, J.C., 2007a. Higher Waves Along U.S. East Coast Linked to Hurricanes. EOS, Transaction of the American Geophysical Union 88 (30), 301. doi:10.1029/2007EO300001.

Komar, P.D., Allan, J.C., 2007b. A note on the depiction and analysis of wave-height histograms. Shore & Beach 75 (3), 1–5.

Komar, P.D., Allan, J.C., 2008. Increasing hurricane-generated wave heights along the U.S. Atlantic Coast and their climate controls. Journal of Coastal Research 24 (2), 479–488. doi:10.2112/07-0894.1.

Komar, P.D., Allan, J.C., Ruggiero, P., 2009. Ocean wave climates: trends and variations due to Earth's changing climate. In: Kim, Y.C. (Ed.), Handbook of Coastal and Ocean Engineering. World Scientific Publishing Co, pp. 971–975.

Longuet-Higgins, M.S., 1952. On the statistical distribution of the heights of sea waves. Journal of Marine Research 11, 245–266.

Mendez, F.J., Menendez, M., Luceño, A., Losada, I.J., 2006. Estimation of the long-term variability of extreme significant wave height using a time-dependent peak over threshold (POT) model. Journal of Geophysical Research 111, C07024. doi:10.1029/2005JC003344.

Mendez, F.J., Menendez, M., Luceño, A., Medina, R., Graham, N.E., 2008. Seasonality and duration in extreme value distributions of significant wave height. Ocean Engineering 35, 131–138.

Menendez, M., Mendez, F.J., Losada, I., Graham, N.E., 2008a. Variability of extreme wave heights in the northeast Pacific Ocean based on buoy measurements. Geophysical Research Letters 35, L22607. doi:10.1029/2008GL035394.

Menendez, M., Mendez, F.J., Izaguirre, C., Luceno, A., Losada, I., 2008b. The influence of seasonality on estimating return values of significant wave height. Coastal Engineering. doi:10.1016/j.coastaleng.2008.07.004.

National Data Buoy Center (NDBC), 2008. National Data Buoy Center, National Oceanographic and Atmospheric Administration. http://seaboard.ndbc.noaa.gov/ (accessed April 1, 2008).

Ochi, K., 1992. New approach for estimating the severest sea state from statistical data. Proceedings of the 23rd International Conference on Coastal Engineering. ASCE, Venice, Italy. 512–525.

Stefanakos, C., Athanassoulis, G.A., 2006. Extreme value predictions based on nonstationary time series of wave data. Environmetrics 17, 25–46.

Wigley, T.M.L., 1988. The effect of changing climate on the frequency of absolute extreme events. Climate Monitor 17, 44–55.

Zhang, X., Zwiers, F.W., Guilong, L., 2004. Monte Carlo experiments on the detection of trends in extreme values. Journal of Climate 17, 1945–1952.

Zwiers, F.W., Kharin, V.V., 1998. Changes in the extremes of the climate simulated by CCC GCM2 under CO_2 doubling. Journal of Climate 11, 2200–2222.